Наносистеми, наноматеріали, нанотехнології
Nanosistemi, Nanomateriali, Nanotehnologii
2023, т. 21, № 2, сс. 233–246

PACS numbers: 71.10.Pm, 74.10.+v, 74.81.Bd, 75.30.Et, 75.30.Kz, 75.47.Gk, 75.47.Lx

Two Types of Topological Kosterlitz–Thouless Phase Transitions in $SmMnO_{3+\delta}$ Manganites, Driven by External Magnetic Field

F. M. Bukhanko

Donetsk Institute for Physics and Engineering Named after O. O. Galkin, N.A.S. of Ukraine,
46 Nauky Ave.,
UA-03028 Kyiv, Ukraine

It is shown that, in a $SmMnO_{3+\delta}$ sample cooled in a magnetic field $H = 0$ to 4.2 K, the topological order–disorder phase transition of the spin system occurs within the framework of the Kosterlitz–Thouless XY-model decoupling of pairs of the flat $2D$ vortices. At the same time, when the sample is cooled in the field $H \neq 0$, the transition of the system of spins to a disordered state with increasing temperature occurs in the form of dissociation of pairs of bounded Z_2 vortices at the same critical temperature $T_{KT} = 12$ K, which is accompanied by a giant jump in the supermagnetization of the sample. The excitation and decay of low-energy bosons in a $1D$ metallic Luttinger liquid at temperatures of 0.5 K and 4.2 K during sample remagnetization in the ZFC and FC measurement modes is also studied.

В даній роботі показано, що в зразку $SmMnO_{3+\delta}$, охолодженому в магнетному полі $H = 0$ до 4,2 К топологічний фазовий перехід лад–безлад спінової системи відбувається в рамках XY-моделю Костерліца–Таулесса дисоціяції пар пласких $2D$-вихорів. Водночас за охолодження зразка у полі $H \neq 0$ перехід системи спінів у невпорядкований стан із підвищенням температури відбувається у вигляді дисоціяції пар зв'язаних Z_2-вихорів за однакової критичної температури $T_{KT} = 12$ К, що супроводжується гігантським стрибком надмагнетованости зразка. Досліджено також збудження та розпад низькоенергетичних бозонів у Латтінґеровій $1D$-металевій рідині за температур у 0,5 К та 4,2 К під час перемагнетування зразка в ZFC- та FC-режимах міряння.

Key words: Kosterlitz–Thouless phase transition, Luttinger liquid, bosons, topological superconductors.

Ключові слова: $2D$-Майоранові пласкі зони, квантування за Ландау, Z_2-кіральна квантова спінова рідина, калібрувальне поле спектру спінонних пар, топологічні надпровідники.

(Received 23 September, 2022)

1. INTRODUCTION

Recently, the Tomonaga–Luttinger liquid model, or simply the Luttinger liquid (LL), has been of great interest. This model describes well the interaction of electrons or other fermions in a one-dimensional conductor. Such a model is necessary because the commonly used Fermi liquid model loses its applicability in the one-dimensional case. The LL theory describes low-energy collective excitations in a one-dimensional electron gas as bosons. The Hamiltonian for free electrons is split over electrons with opposite (left–right) directions of motion. Among the physical systems described by this model, there are: conduction electrons in the mode of fractional or integer quantum Hall effect, $1D$ chains of half-integer spins described by the Heisenberg model. The LL theory describes well the low-energy properties of a wide class of gapless one-dimensional interacting fermionic systems [1, 2].

The limitation of consideration to low excitation energies is usually justified by the linearization of the spectrum of physical fermions around the right and left Fermi points $\epsilon(k) \approx v_F (\pm k \quad k_F)$. Within this approximation, the system can be rigorously described even in the presence of nonzero interactions between particles. The theory of interacting fermions is transformed into the theory of non-interacting bosons, and all correlation functions can be calculated exactly. It is assumed that in the one-dimensional case, excitations of many particles in the form of charge and spin density waves, which obey Bose statistics, mainly replace the elementary excitations of fermions. One of the remarkable features of one-dimensional conducting systems of fermions in the Luttinger liquid state is the separation of spins and charges. The Hamiltonian of the interacting system is divided into two commuting terms, which act in different Hilbert spaces, describe the charge, and spin degrees of freedom separately. This unusual state of one-dimensional conducting systems is completely characterized by the spin and charge density wave velocities (v_s and v_c, respectively) and the Luttinger parameter K, which depends on the magnitude of the interaction between the particles. For nonzero interactions, these rates differ. The collective nature of the LL Eigen oscillations and the existence of separation of spins and charges are clearly manifested in various dynamic response functions. The structure factors of charge density $S(k, \omega)$ and spin $S^{-+}(k, \omega) = S^x \pm iS^y$, $S^{zz}(k, \omega)$ measure the linear response of a system of particles with momentum k and energy ω to a perturbation that changes the density of charges and spins in the system. For a spin LL, the dynamic structure factor of the charge density is $S(k, \omega) \propto \delta(\omega - v_c|k|)$, while the dynamic structure factor of the spin density is $S^{zz}(k, \omega) = 1/2S^{-+}(k, \omega) \propto \delta(\omega - v_s|k|)$. The presence of the δ-shaped Dirac peak of these functions reflects the fact that the charge and spin waves are natural oscillations of the LL; therefore, each value of the wave number corresponds to certain excitation energy. This result is directly related to the linearization of the fermion spectrum in the linear LL theory. It should be noted that, according to this model, charge and spin density waves are completely decoupled. Far from the Fermi points, the curvature of the physical spectrum of fermions $\epsilon(k)$ cannot be neglected, for example, curvature of the fermion spectrum leads to coupling of charge and spin density waves [3–5].

In Refs. [6, 7], the dynamic response of strongly correlated one-dimensional Mott insulators with a spectral gap M with a half and a quarter filling level of the conduction band was considered. It was found that the dynamic response functions of charges and spins are very different in these two cases. According to [6], in the limit of low excitation energies, both systems exhibit spin-charge separation, which made it possible to accurately calculate their dynamic spectral function of the charge density and spin $A(\omega, k_F + q)$. It was found that, in a one-dimensional half-filled Mott dielectric at a temperature $T = 0$ K, the excitation and annihilation operators of an ensemble of left-handed and right-handed fermions separate them into separate charge and spin fragments as a result of bosonization in the form of charge and spin density waves. The paper presents a series of spectral functions $A_R(\omega, k_F + q)$ calculated for the cases $v_s = 0.8v_c$, $-4M \le q \le 4M$, which clearly shows the existence of two peaks corresponding to CDW and SDW excitation. Much of the spectral weight is concentrated in these features, which are a direct manifestation of the charge-spin separation. The peak feature of the spectral function with a lower (higher) energy corresponds to a situation in which all fermions with momentum q participating in the formation of the collective continuum of excitations are spin (charge) carriers. It is important to note that both peaks have a significant width. At low temperatures $T < M$, the effect of temperature increase on the charge correlation function is small, but the spin part of the spectral function can change greatly, since there is no gap in the spinon spectrum. It was found that the spectral function of a one-dimensional Mott dielectric with a quarter-filling level does not contain two distinct peak features associated with separate excitation of charge and spin density waves. In contrast to half-filling, one can expect the presence of only one asymmetric very wide dispersed peak in the density of states $A(\omega, k_F + q)$ located around k_F. The formation of low-energy bosons in the form of $1D$

charge/spin density waves in systems of AFM spin chains, caused by confinement of spinon pairs, has been well studied in [8–14].

As shown in [15–17], the formation of ultranarrow $2D$ bands of Majorana fermions in graphene as a result of Landau quantization of the spectrum of quasi-particles with the Dirac spectrum of collective excitations is a possible reason for the appearance of topological superconductivity in graphene. In [15], the superconducting properties of a two-dimensional Dirac material, such as deformed graphene, which in normal state has a spectrum of free charge carriers with a flat energy band. It is shown that in the superconducting state, the appearance of a flat energy band of carriers caused by deformation leads to a strong increase in the critical temperature of superconductivity compared to the case without deformation, an inhomogeneous order parameter with a two-peak shape of the local density of states, and a large, almost uniform and isotropic supercurrent. According to [16], in systems with a condensed state, when a quasiparticle is a superposition of electron and hole excitations and its production operator $\gamma^\dagger$ becomes identical to the annihilation operator γ, such a particle can be identified as a Majorana fermion. In the Reed–Green model, the Bogolyubov quasi-particles in the volume become dispersive Majorana fermions, and the bound state formed in the core of the vortex becomes the Majorana zero mode. The former is interesting as a new type of wandering quasiparticles, while the latter is useful as a qubit for topological quantum computing. Thus, the formation of flat bands of Majorana fermions is a characteristic mechanism of topological superconductivity, BCS and Bose–Einstein condensation of bosons in the form of a bound state of $2D$ Majorana fermions and Dirac superconducting flat zone. The crossover of electron pairs characteristic of BCS and Bose–Einstein condensation of bosons in the form of a bound state of Majorana fermions (Majorana zero mode) was also studied in topological superconductors.

2. EXPERIMENTAL TECHNIQUE

Samples of self-doped manganites $SmMnO_{3+\delta}$ ($\delta \cong 0.1$) were obtained from high-purity oxides of lanthanum, samarium and electrolytic manganese, taken in a stoichiometric ratio. The synthesized powder was pressed under pressure of 10 kbar into discs of 6 mm in diameter, 1.2 mm thick and sintered in air at a temperature of 1170°C for 20 h followed by a decrease in temperature from at a rate of 70°C/h. The resulting tablets were is a single-phase ceramic according to x-ray data. X-ray studies were carried out with 300 K on DRON-1.5 diffractometer in radiation $NiK_{\alpha_1+\alpha_2}$. Symmetry and parameters of the crystal gratings were determined by the position and character splitting reflections of the pseudocubic lattice perovskite type. Temperature and field dependences of magnetization were obtained in ZFC- and FC-measurement modes *dc* magnetization in the range of fields -5 kOe $\leq H \leq 5$ kOe at 4.2 K using a non-industrial magnetometer.

2. EXPERIMENTAL RESULTS AND DISCUSSION

According to the results of studying the temperature dependences of the magnetization dc in $SmMnO_{3+\delta}$ measured in the FC mode [18–20], in the temperature range $0 < T \leq 20$ K, the magnetization contains three contributions: the well-known dominant contribution of the magnetization of the Z_2 RVB phase of the gap quantum spin liquid in the form of a broad magnetization peak with a top near 20 K and weaker additional contributions to the magnetization of the degenerate state of thermal excitations of the spinon and vortex pairs in the form of characteristic features of the supermagnetization of samples near temperatures $T_{spinon} \cong 8$ K and $T_{KT} \cong 12$ K, where T_{spinon} is the average temperature of thermal excitation of the spinon spectrum in QSL, and T_{KT} is the temperature of the topological Kosterlitz–Thouless phase transition of the dissociation of 2*D* vortex pairs in a superconducting quantum liquid. In the FC measurement mode, the QSL is in a polarized state, which makes it possible to record weak changes in the magnetization of the samples induced by thermal excitations of the nonmagnetic (singlet) ground state of the quantum spin liquid in $SmMnO_{3+\delta}$ in the region of very low temperatures.

According to Fig. 1, the excitation of spinons with $S = $ S in a magnetic field $H = 100$ Oe occurs mainly in the temperature range 6–10 K in the form of a doublet of two broad almost overlapping supermagnetization peaks of the samples near the average excitation temperature $T_{spinon} \cong 8$ K, which corresponds to the thermal excitation energy of $E_{spinon} \cong 0.6$ meV. At temperatures below 6 K, two weak magnetization doublets of spinon pairs are observed, with an excitation energy E_{spinon} lower than the low-energy gap $\Delta_s \approx 0.4$ meV in the spinon excitation spectrum existing in the 2*D* system of spins between the nonmagnetic singlet spin state in the ground RVB state of the QSL and the excited magnetic state in the form of spinons. As can be clearly seen from Fig. 1, the doublet excitation of spinon pairs with $S = 1/2$ occurs in the temperature range that overlaps with the temperatures of decoupling of pairs of 2*D* vortices of the superconducting liquid, which indicates the practical coincidence (crossover) of their excitation energies. The decoupling of vortex–antivortex pairs in a superconducting liquid at temperatures above T_{KT} is accompanied by a giant jump in the supermagnetiza-

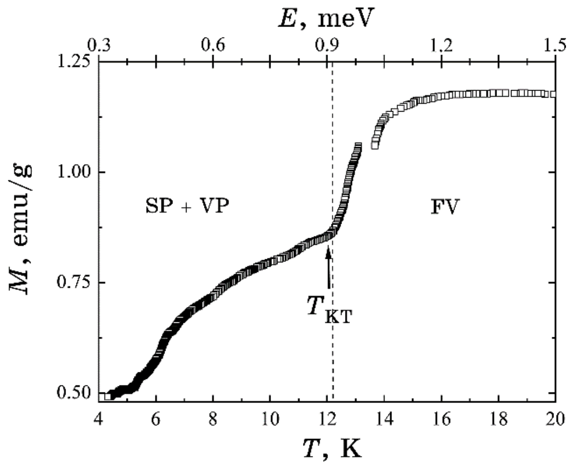

Fig. 1. The temperature dependence $M(T)$ of mixed state spin and superconducting quantum liquids in $SmMnO_{3+\delta}$ in FC mode, measured in the field $H = 100$ Oe in the temperature range 4.2–20 K. At temperatures $T \geq T_c = T_{KT} \cong 12$ K, a strong jump of the magnetization curve $M(T)$ is observed, caused by a topological phase transition of the dissociation of Z_2 vortex–antivortex pairs in a superconducting quantum liquid [spinon pairs (SP), vortex pairs (VP), free vortices (FV)].

tion of the sample.

The jump in magnetization is explained by the appearance of plasma of free 2*D* vortices in the SC of a quantum liquid with the opposite direction of magnetic moments, which are easily oriented along the direction of the external magnetic field. Thus, in weak magnetic fields of ≅ 100 Oe, the thermal excitation energies of pairs of spinons with $S = 1/2$ and the plasma of 2*D* electron vortices practically coincide, which indicates the degeneracy of the ground states of spin and superconducting quantum liquids. As can be seen from Fig. 1, the jump in the additional magnetization near the T_{KT} is almost three times greater than its increase near T_{spinon}, which indicates a more significant contribution of the free vortex magnetization to the total magnetization of the sample.

Figure 2 clearly show that an increase in the strength of an external magnetic field to the value $H = 1$ kOe leads to significant changes in the temperature dependences of the $M(T)$ curves near the critical temperature T_{KT} of transition into a coherent superconducting state. First, there is a complete consolidation of two weakly resolved peaks of doublet excitation of spinon pairs with $S = 1/2$ into a single symmetric sinus-like peak near the average temperature $T_{spinon} \cong 8$ K and a strong broadening of the spinon excitation spectrum in the temperature range 6–10 K. This result evidences of

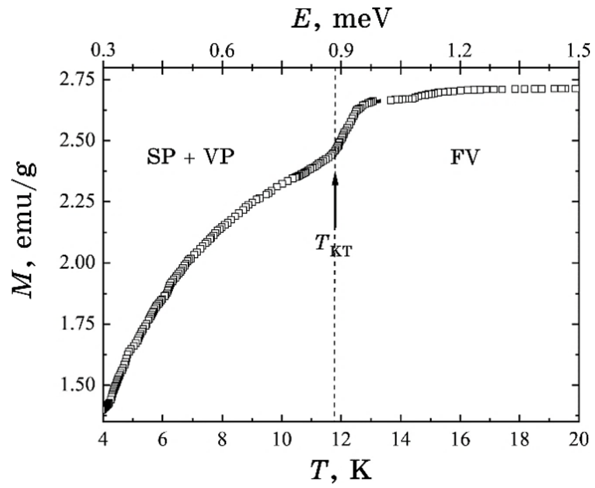

Fig. 2. The temperature dependence $M(T)$ of mixed state spin and superconducting quantum liquids in $SmMnO_{3+\delta}$ in FC mode, measured in the field $H = 1$ kOe in the temperature range 4.2–20 K. At temperatures $T_{KT} \cong 12$ K, a strong decrease of the jump of supermagnetization is observed [spinon pairs (SP), vortex pairs (VP), free vortices (FV)].

the existence of 'gigantic' fluctuations arising in the ground state of QSL, which leads to smearing of the spectrum of low-energy spinon excitations. Secondly, the growth of the external magnetic field leads to a strong decrease of the jump of supermagnetization near the critical temperature $T_{2D} \equiv T_{KT} \cong 12$ K of the $2D$ vortex pairs' dissociation, while the intensity of spinon pair excitation near $T_{spinon} \cong$ $\cong 8$ K is practically unchanged. This indicates that the QSL is much more stable to the action of an external magnetic field compared to the coherent SC state. Further destruction of the coherent SC state in the superconducting composite occurs in the magnetic field $H = 3.5$ kOe (Fig. 3).

This manifests itself in the almost complete suppression of the 'gigantic' jump in supermagnetization near $T_{KT} \cong 12$ K. Only a weak jump in the temperature dependence of magnetization is observed near T_{KT}, separating the phase with new quantum spinon oscillations and the phase with a low density of bonded vortex-antivortex pairs. A distinctive feature of the temperature dependences of the supermagnetization $M(T)$, obtained with increasing external magnetic field up to 3.5 kOe, is the appearance of clearly pronounced stepped oscillations of the spinon gas magnetization. As is clearly shown in Fig. 3, a characteristic feature of the supermagnetization oscillating in the temperature range of 4.2–9 K is the appearance of periodic threshold features of width $\Delta E \cong 0.08$–0.15 meV with char-

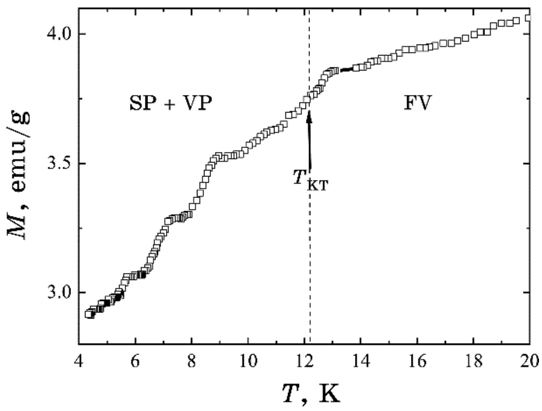

Fig. 3. The temperature dependence $M(T)$ of mixed state spin and superconducting quantum liquids in $SmMnO_{3+\delta}$ in FC mode, measured in the field $H = 3.5$ kOe in the temperature range 4.2–20 K. At temperatures $T_{KT} \cong 12$ K, a further destruction of the coherent SC state in the superconducting composite is observed [spinon pairs (SP), vortex pairs (VP), free vortices (FV)].

acteristic narrow plateaus in the temperature dependence of the sample magnetization in Landau bands with $n = 1$, $n = 2$, and $n = 3$. With increasing T, the height of thresholds and width of steps (plateaus) grow. New quantum oscillations of temperature dependences of the 'supermagnetization' of $2D$ spinon gas in the form of three narrow steps (plateaus) correspond to an integer filling of three finite gap Landau levels with spinons in a strong external magnetic field. Thus, even a relatively small increase in the strength of the external magnetic field led to the almost complete destruction of the coherent SC state and the transition from a continuous spinon excitation spectrum of the QSL to a discrete one. Note the significant difference in the evolution of the Landau quantization of the spectrum of spinon pairs in $SmMnO_{3+\delta}$ and $La_{0.15}Sm_{0.85}MnO_{3+\delta}$ with an increase in the strength of the external magnetic field.

In this work, the excitation and decay of low-energy bosons in $SmMnO_{3+\delta}$ at temperatures of 0.5 K and 4.2 K during sample remagnetization in the ZFC and FC measurement mode was also studied. Figure 4 shows the field dependences $M(H)$ of the magnetization of $SmMnO_{3+\delta}$ at $T = 0.6$ K in the ZFC measurement mode in the form of magnetization isotherms—*1* and remagnetization—*2*. As can be seen from the figure, two peak features are formed during sample magnetization $M(H)$ of equal intensity near $H_1 \cong -300$ Oe and $H_2 \cong 0$ in the interval of magnetic fields ±600 Oe, which are characteristic of the excitation of decoupled $1D$ charge and spin

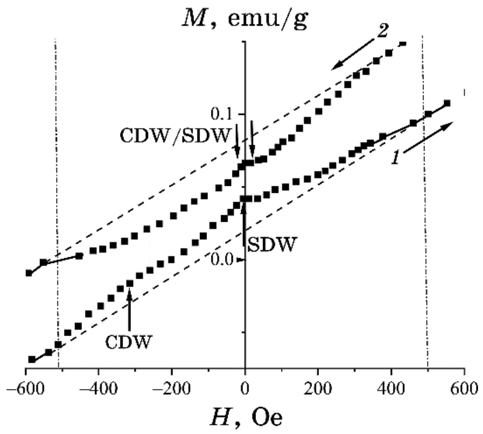

Fig. 4. Isotherms of magnetization—*1* and remagnetization—*2* of the sample $SmMnO_{3+\delta}$ in ZFC mode in the range of magnetic fields ±600 Oe at temperature $T = 0.6$ K. Two-peak features are formed during sample magnetization $M(H)$ of equal intensity near $H_1 \cong -300$ Oe and $H_2 \cong 0$, which are characteristic of the excitation of decoupled 1*D* charge and spin density waves in a Luttinger liquid.

density waves in a Luttinger liquid [2].

It should be noted that, according to the experimental results obtained in this work, in magnetization isotherm *1* at a sample temperature of 0.6 K, decoupled charge and spin density waves are formed, which are characteristic of the excitation of a 1*D* metallic Luttinger liquid. While in remagnetization isotherm *2* near zero magnetic field, a coupled 1*D* CDW/SDW appears in the form a wide magnetization trough $M(H)$. This unusual state is similar to the excitation of two coupled 1*D* Majorana zero modes—characteristic of collective excitations of topological superconductors. The excitation of such collective 1*D* states in an external magnetic field was observed earlier in systems weakly coupled by the exchange of Heisenberg and Ising AFM spin chains with different configurations and degrees of anisotropy [8–14].

According to these works, even a weak increase in the transverse component of the external magnetic field can lead to further confinement of spinon pairs, which is accompanied by the appearance of gapless modes of natural longitudinal oscillations of the system of spin chains. As can be seen in Fig. 5, a slight increase in the temperature of $SmMnO_{3+\delta}$ to 4.2 K led to a dramatic change in the magnetization reversal isotherms of the sample. There was a splitting of the peak features of the supermagnetization $M(H)$ on isotherm *1* near the critical values of the external magnetic field strength H_1 and H_2, which we associate with the excitation of

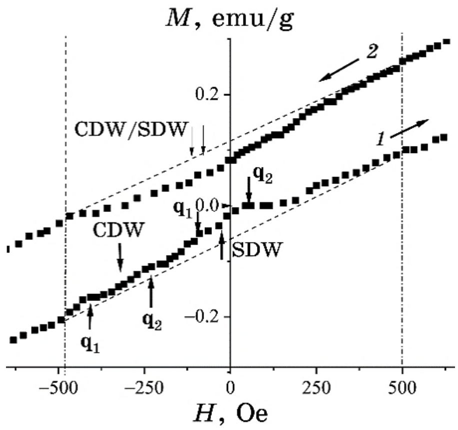

Fig. 5. Isotherms of magnetization—*1* and remagnetization—*2* of the sample $SmMnO_{3+\delta}$ in ZFC mode in the range of magnetic fields ±600 Oe at temperature $T = 4.2$ K. A splitting of the peak features of the supermagnetization $M(H)$ on isotherm *1* near the critical values of the external magnetic field strength $H_1 \cong -300$ Oe and $H_2 \cong 0$, associated with the excitation of fragments of decoupled charge and spin density waves with different wave vectors $\mathbf{q}_1$ and $\mathbf{q}_2$.

fragments of decoupled charge and spin density waves with different wave vectors $\mathbf{q}_1$ and $\mathbf{q}_2$ parallel to the *a* and *b* axes of the crystal lattice. At the same time, the splitting of a wide magnetization trough $M(H)$ near zero field at $T = 0.6$ K completely disappeared with increasing temperature, which can be explained by the strengthening of the coupling of two 1*D* Majorana modes and a strong increase in charge/spin fluctuations. According to Fig. 6, during the remagnetization of the $SmMnO_{3+\delta}$ sample at 4.2 K in the FC mode, the field dependences $M(H)$ of the magnetization practically coincide with the measured dependences of the magnetization at $T = 0.6$ K in the ZFC mode. This indicates a higher stability of low-energy boson excitations in this measurement mode.

It is known that in two-dimensional (2*D*) systems at all temperatures spontaneous ordering with the appearance of a conventional long-range order is impossible. Studies of critical behaviour within the framework of the classical two-dimensional *XY* model have shown that at sufficiently low temperatures, a phase with new properties arises in a 2*D* system, in which there is no conventional long-range order. A number of theories predict a low-temperature region, which is characterized as a phase of critical points with continuously changing critical indices. Within this phase, the correlation functions of the order parameter decrease at large distances according to power laws, while at temperatures above the critical

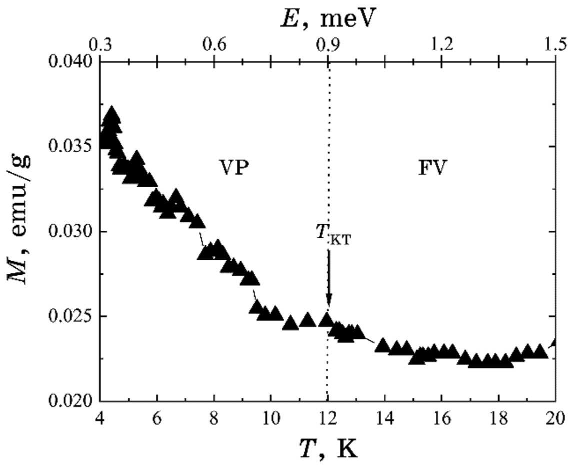

Fig. 6. Isotherms of magnetization—*1* and remagnetization—*2* of the sample $SmMnO_{3+\delta}$ in FC mode in the range of magnetic fields ±600 Oe at temperature $T = 4.2$ K. Two-peak features are formed during sample magnetization $M(H)$ near $H_1 \cong -300$ Oe and $H_2 \cong 0$ with different intensity, which are characteristic of the excitation of decoupled 1*D* charge and spin density waves in a Luttinger liquid.

value, the correlations decay exponentially. Kosterlitz and Thouless predicted a new phase transition order–disorder type in a two-dimensional lattice of spins, which is characterized by the establishment of a topological long-range order in a flat system [22–24].

According to the *XY* Kosterlitz–Thouless model, the decoupling of 2*D* vortex pairs is accompanied by a cusp-shaped drop in the two-dimensional density of neutral superfluid liquids or the critical current density in two-dimensional networks of Josephson weak links. Previously, we discovered in $SmMnO_{3+\delta}$ a cusp-shaped feature of the magnetization curves $M(T)$ in the ZFC measurement mode near the critical temperature of the Kosterlitz–Thouless transition of the sample to the coherent superconducting state $T_{KT} \equiv T_c \cong 12$ K, which is characteristic of the dissociation of 2*D* vortex pairs (Fig. 7). In a narrow range of low temperatures $8\text{ K} < T < 12\text{ K}$, a plateau was found in the temperature dependence of the dc magnetization of the sample, while in the higher temperature range $12\text{ K} < T < 16\text{ K}$, the magnetization decreases exponentially. This result differs significantly from the behaviour of the magnetization $M(T)$ near T_{KT} measured in $SmMnO_{3+\delta}$ in FC mode (Fig. 1).

In Ref. [25], the nature of the Kosterlitz–Thouless phase transition has been studied within the framework of the Heisenberg model with the exchange integral *J*. The model is based on the concept of a topologically stable point defect—the Z_2 vortex. Unlike an or-

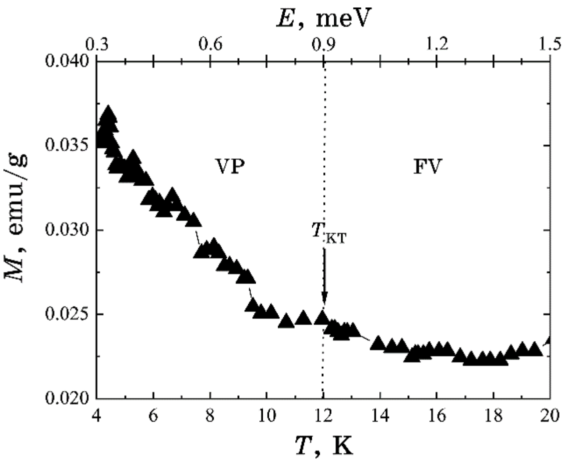

Fig. 7. A cusp-shaped feature of the magnetization curves $M(T)$ in $SmMnO_{3+\delta}$ in the ZFC measurement mode near the critical temperature of the Kosterlitz–Thouless transition of the sample to the coherent superconducting state $T_{KT} \equiv T_c \cong 12$ K, which is characteristic of the dissociation of $2D$ vortex pairs [vortex pairs (VP), free vortices (FV)].

dinary $2D$ vortex, which is considered in the two-dimensional XY model, Z_2 vortices are characterized by a topological quantum number. Just like ordinary vortices, Z_2 vortices at low temperatures exist in the form of a bound pair and begin to dissociate at a certain critical temperature, which corresponds to the Kosterlitz–Thouless phase transition. In contrast to the XY model, in this model the spin waves destroy the spin order in such a way that the spin correlation decreases exponentially even in the low-temperature phase. Therefore, the Kosterlitz–Thouless-like phase transition occurs between two phases with exponential decay of spin correlations.

The authors found that the 'order parameter', which characterizes the low-temperature and high-temperature phases, could be introduced through the vorticity function of the system of spins, which has the structure of a Wilson loop in the gauge theory. At low temperatures, Z_2 vortices exist only as strongly coupled pairs of vortices. At temperatures above T_{KT}, one can expect spontaneous generation of free Z_2 vortices. The same transition was proposed by Kosterlitz–Thouless for ordinary $2D$ vortices within the framework of the XY model. The question arises as to which physical parameter makes it possible to qualitatively distinguish between the low-temperature and high-temperature Z_2 phases. Such a parameter is the vorticity function $V[C]$ on the contour C, whose thermal averaging over the contour C is the topological order parameter $V_R = \langle V_R[C] \rangle$, where R is the perimeter of the contour. The temperature dependence of the heat capacity exhibits a sharp peak near the temperature $T/J = 0.3$, which corresponds to the critical temperature of the Kosterlitz–Thouless topological phase transition decoupling Z_2 of vortex pairs. The temperature dependence of the density of elementary Z_2 vortices $n_v(T)$ exhibits a sharp decrease in n_v with decreasing temperature near the maximum heat capacity. A simulation of the Z_2 distribution of vortex pairs in the lattice plane at temperatures below and above the T_{KT} is given. As expected, at low temperatures, Z_2 vortices are tightly coupled vortex pairs. As the temperature rises, both the number Z_2 of vortex pairs and the separation between the vortices forming a pair increase. At $T/J = 0.32$, pairs of vortices appear with a separation much greater than the period of the crystal lattice, which confirms the mechanism of decoupling of vortex pairs during the Kosterlitz–Thouless transition. It should be noted that there is a tendency for the formation of clusters from $N > 2$ vortex pairs. At $T/J = 0.34$, the density of elementary Z_2 vortices $n_v(T)$ increases strongly. Z_2 vortex in this model can be considered as a vortex formed by chirality vectors.

4. CONCLUSION

In this paper, it is shown that in a $SmMnO_{3+\delta}$ sample cooled in a magnetic field $H = 0$ to 4.2 K (ZFC mode), the topological order–disorder phase transition of the spin system occurs within the framework of the XY Kosterlitz–Thouless model: decoupling of pairs of the flat $2D$ vortices, which is accompanied by cusp-like drop in the two-dimensional density of neutral superfluid liquid or the critical current density in two-dimensional networks of Josephson weak links. At the same time, when the sample is cooled in the field $H \neq 0$ (FC mode), the transition of the system of spins to a disordered state with increasing temperature occurs in the form of dissociation of pairs of bounded Z_2 vortices at the same critical temperature $T_{KT} = 12$ K, which is accompanied by a giant jump in the supermagnetization of the sample.

REFERENCES

1. F. D. M. Haldane, *Phys. Rev. Lett.* **47**, 1840 (1981); https://doi.org/10.1103/PhysRevLett.47.1840
2. T. L. Schmidt, A. Imambekov, and L. I. Glazman, *Phys. Rev. B*, **82**: 245104 (2010); https://doi.org/10.48550/arXiv.1009.4708
3. S. Brazovskii, F. Matveenko, and P. Nozieres, *JETP Letters*, **58**: 796 (1993); doi: 10.1051/jp1:1994161
4. T. Vekua, S. I. Matveenko, and G. V. Shlyapnikov, *JETP Letters*, **90**: 289 (2009); https://doi.org/10.1134/S0021364009160139

5. M. Rizzi, M. Polini, M. A. Cazalilla, M. R. Bakhtiari, M. P. Tosi, and R. Fazio, *Phys. Rev. B*, **77**: 245105 (2008); https://doi.org/10.1103/PhysRevB.77.245105
6. Fabian H. L. Essler and Alexei M. Tsvelik, *Ann. Henri Poincaré*, **4**, Suppl. 2: S589 (2003); doi:10.1007/s00023-003-0945-7
7. D. Controzzi and F. H. L. Essler, *Phys. Rev. B*, **66**: 165112 (2002); https://doi.org/10.1103/PhysRevB.66.165112
8. W. J. Gannon, I. A. Zaliznyak, L. S. Wu, A. E. Feiguin, A. M. Tsvelik, F. Demmel, Y. Qiu, J. R. D. Copley, M. S. Kim, and M. C. Aronson, *Nature Communications*, **10**: 1123 (2019); https://doi.org/10.1038/s41467-019-08715-y
9. Bella Lake, Alexei M. Tsvelik, Susanne Notbohm, D. Alan Tennant, Toby G. Perring, Manfred Reehuis, Chinnathambi Sekar, Gernot Krabbes, and Bernd Büchner, *Nature Physics*, **6**: 50 (2010); doi:10.1038/nphys1462
10. Zhe Wang, M. Schmidt, A. K. Bera, A. T. M. N. Islam, B. Lake, A. Loidl, and J. Deisenhofer, *Phys. Rev. B*, **91**: 140404 (R) (2015); https://doi.org/10.1103/PhysRevB.91.140404
11. B. Grenier, S. Petit, V. Simonet, E. Canevet, L.-P. Regnault, S. Raymond, B. Canals, C. Berthier, and P. Lejay, *Phys. Rev. Lett.*, **114**: 017201 (2015); https://doi.org/10.1103/PhysRevLett.114.017201
12. M. Matsuda, H. Onishi, A. Okutani, J. Ma, H. Agrawal, T. Hong, D. M. Pajerowski, J. R. D. Copley, K. Okunishi, M. Mori, S. Kimura, and M. Hagiwara, *Phys. Rev. B*, **96**: 024439 (2017); https://doi.org/10.1103/PhysRevB.96.024439
13. Q. Faure, S. Takayoshi, S. Petit, V. Simonet, S. Raymond, L.-P. Regnault, M. Boehm, J. S. White, M. Mensson, C. Rьegg, P. Lejay, B. Canals, T. Lorenz, S. C. Furuya, T. Giamarchi, and B. Grenier, *Nature Physics*, **14**: 716 (2018); https://doi.org/10.1038/s41567-018-0126-8
14. A. K. Bera, B. Lake, F. H. L. Essler, L. Vanderstraeten, C. Hubig, U. Schollwöck, A. T. M. N. Islam, A. Schneidewind, and D. L. Quintero-Castro, *Phys. Rev. B*, **96**: 054423 (2017); https://doi.org/10.1103/PhysRevB.96.054423
15. V. J. Kauppila, F. Aikebaier, and T. T. Heikkilä, *Phys. Rev. B*, **93**: 214505 (2016); https://doi.org/10.1103/PhysRevB.93.214505
16. M. Sato and Y. Ando, *Rep. Prog. Phys.*, **80**: 076501 (2017); https://doi.org/10.1088/1361-6633/aa6ac7
17. L. Balents, C. R. Dean, D. K. Efetov, and A. F. Young, *Nature Physics*, **16**: 725 (2020); https://doi.org/10.1038/s41567-020-0906-9
18. F. N. Bukhanko and A. F. Bukhanko, *Nanosistemi, Nanomateriali, Nanotehnologii*, **16**, Iss. 2: 271 (2018); https://doi.org/10.15407/nnn.16.02.271
19. F. N. Bukhanko and A. F. Bukhanko, *Fizika Nizkikh Temperatur*, **47**: 1021 (2021); doi:10.1063/10.0006569
20. F. N. Bukhanko and A. F. Bukhanko, *Fizika Tverdogo Tela*, **64**: 181 (2022); doi:10.21883/FTT.2022.02.51928.142
21. F. N. Bukhanko and A. F. Bukhanko, *Journal of Technical Physics*, **61**: 1531 (2016); https://doi.org/10.1134/S1063784216100091
22. J. M. Kosterlitz and D. J. Thouless, *J. Phys. C*, **5**: L124 (1972); https://doi.org/10.1088/0022-3719/5/11/002
23. J. M. Kosterlitz and D. J. Thouless, *J. Phys. C*, **6**: 1181 (1973); https://doi.org/10.1088/0022-3719/6/7/010
24. J. M. Kosterlitz, *J. Phys. C*, **7**: 1046 (1974); https://doi.org/10.1088/0022-3719/7/6/005
25. H. Kawamura and S. Miyashita, *J. Phys. Soc. Jap.*, **53**: 4138 (1984); https://doi.org/10.1143/JPSJ.53.4138